

The 2nd Asian Nuclear
Reaction Database
Development Workshop

CNDC of CIAE
and
AASPP of JSPS

Beijing, China
September 06., 2011



Bharathiar University
Coimbatore. India.



*A comparison of ternary
fragmentation potential
energy surface in equatorial
and collinear configuration*

M. Balasubramaniam
Assistant Professor
Department of Physics
Bharathiar University
Coimbatore - 641046



This document was prepared as an account of work to present in the 2nd Asian Nuclear Reaction Database Development Workshop

Thanks



Bharathiar University
Coimbatore. India.



THANKS FOR THIS OPPORTUNITY



Our nuclear data activities



Bharathiar University
Coimbatore. India.



In 2008, I got an opportunity to interact with Prof. S. Ganesan in a meeting at Tirunelveli and initiated a project proposal which was later sanctioned and supported by DAE-BRNS, Govt. of India in 2009. (On going)

In 2008 we at BU, attended couple of nuclear data related meetings at Manipal University, Manipal during 25th to 28th February, 2008 and the other one during October 2-4, 2008.

The first meeting was on Covariance error matrices (Prof. Leeb) and in the later meeting Dr. R. Capote conducted a demonstrative program for the use of EMPIRE code.



In 2009, we actively participated in the third DAE-BRNS Theme Meeting on EXFOR Compilation of Nuclear Data, November 03-07, 2009, Jaipur, Rajasthan, India.

Dr. D. Svetlena, IAEA demonstrated about how to make entries in the EXFOR and also about the digitizer software. (Inpgraph)

All the participants with the support of Dr. D. Svetlena and other experts made several entries during that meeting.

Following entries were made by us



ENTRY	D6022
TITLE	Measurement of near and above barrier fusion excitations for 7-Li+28-Si
AUTHOR	H.Majumdar, Mandira, Sinha, P.Basu, R.Bhattacharya, Subinit Roy, S.Santra, M.Biswas, V.V.Parkar, B.R.Behra, K.S.Golda, S.K.Datta, S.Kailas
Compiled by	K. Manimaran, Megha Bhike, C. Karthik
<u>ENTRY</u>	<u>D6062</u>
TITLE	Proton and alpha evaporation spectra in low energy C-12 and O-16 induced reactions
AUTHOR	E.T.Mirgule, D.R.Chakrabarty, V.M.Datar, Suresh Kumar, Mitra, H.H.Oza
Compiled by	Megha Bhike, K. Manimaran, C. Kartik
<u>ENTRY</u>	<u>D6089</u>
TITLE	$^{13}\text{C}(\alpha, \text{neutron})^{16}\text{O}$ reaction cross section between 1.95 and 5.57 MeV
AUTHOR	K.K.Sekheran, A.S.Divatia, M.K.Metha, S.S.Kerekatte, K.B.Nambiar
Compiled by	K. Manimaran, Megha Bhike, C. Karthik
<u>ENTRY</u>	<u>D6021</u>
TITLE	Direct and compound reactions induced by unstable helium beams near the Coulomb barrier
AUTHOR	A.Navin, V.Tripathi, Y.Blumenfeld, V.Nanal, C.Simanel, M.Casandjian, G.de France, R.Raabe, D.Bazin, A.Chatterjee, M.Dasgupta, S.Kailas, R.C.Lemmon, K.Mahata, R.G.Pillay, E.C.Pollacco, K.Ramachandran, M.Rejmund, A.Shrivastava, J.L.Sida, E.Tryggestad
Compiled by	G.Pandikumar, Dr. S. Ganesan, Dr.M.Balasubramaniam, Joseph Jermiah



ENTRY	D6039
TITLE	Complete and Incomplete Fusion Reactions of O-16 with As-75 at Incident Energies below 7MeV/A
AUTHOR	R.Gun, D S.K.Saha
Compiled by	G.Pandikumar, Dr.S.Ganesan, Dr.M.Balasubramaniam, J.Joseph Jeremiah, P.Balaji
ENTRY	D6051
TITLE	Sub-barrier fusion excitation for the system $7\text{Li}+28\text{Si}$
AUTHOR	Mandira Sinha, H.Majumdar, P.Basu, Subinit Roy, R.Bhattacharya, M.Biswas, M.K.Pradhan, S.Kailas
Compiled by	G.Pandikumar, Dr.S.Ganesan, Dr.M.Balasubramaniam, J.JosephJeremiah
ENTRY	D6085
TITLE	REACTION 55-MN(P,N)55-FE FROM EP=1.35 TO 5.42 MEV
AUTHOR	Y.P.Viyogi, P.Satyamurthy, N.K.Ganguly, S.Kailas, S.Saini, M.K.Mehta
Compiled by	G.Pandikumar, Dr.S.Ganesan, Dr. S.Kailas, J.Joseph Jeremiah, Dr.M.Balasubramaniam



In April 2011, Chanidgarh Exfor meeting

Thanks to **GSYS**

We made couple
of entries, In particular
D6121 was coded
by us with 41 subentries

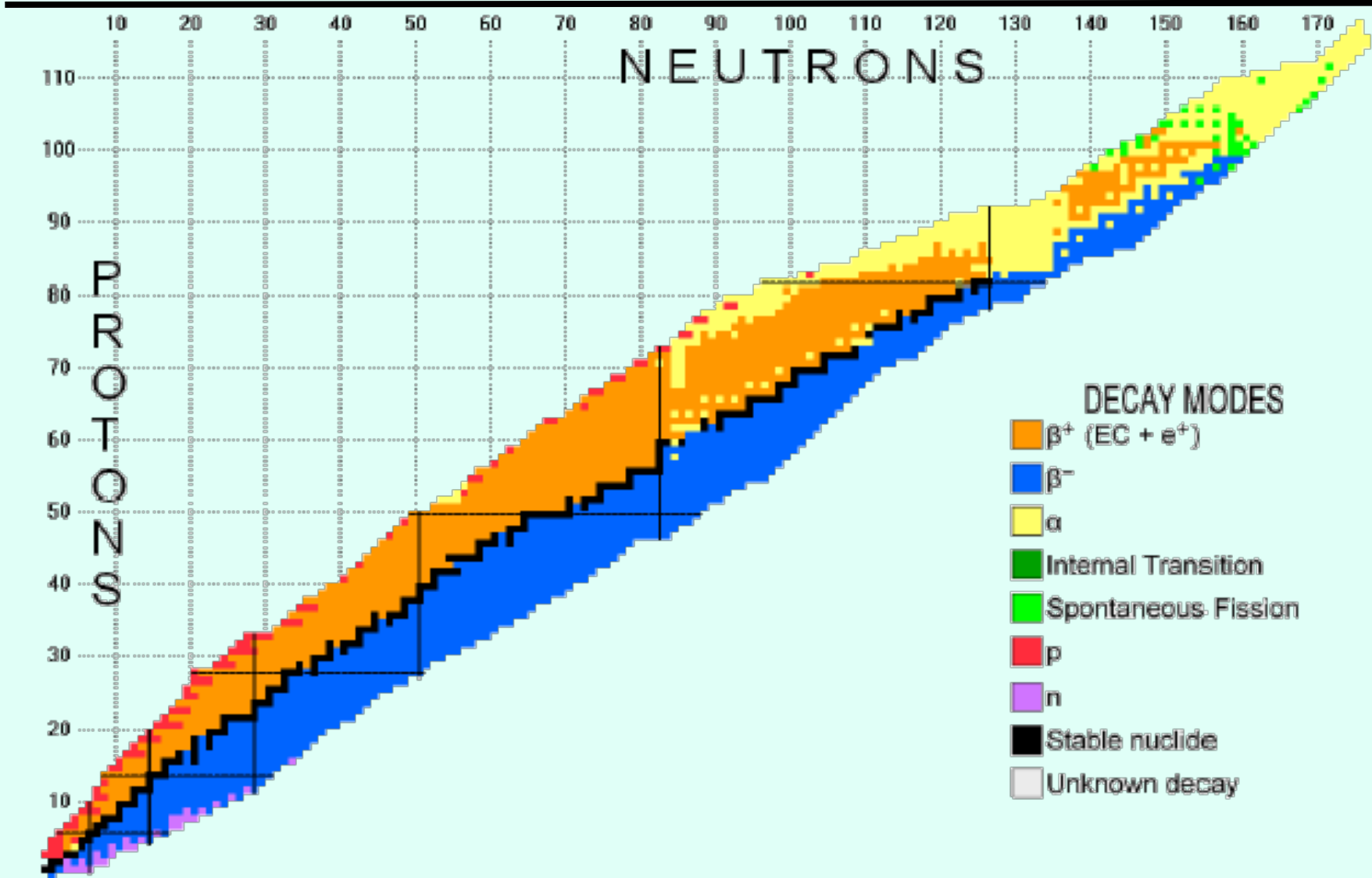
We helped others
To the Exfor, Inpgraph
And Gsys.

```

D6121 - Notepad
File Edit Format View Help
ENTRY          D6121      20110404      D6121  0    1
SUBENT         D6121001  20110404      D6121  1    1
BIB            11          19            D6121  1    2
TITLE          Fission time scale from prescission neutron, proton,
and a particle multiplicities in 28Si+175Lu
AUTHOR         (K.Ramachandran,A.Chatterjee,A.Navin,K.Mahata,
A.Shrivastava, V.Tripathi,S.Kailas,V.Nanal,R.G.Pillay,
A.Saxena,R.G.Thomas, Suresh Kumar,P.K.Sahu)
INSTITUTE      (3INDTRM,3INDTAT)
REFERENCE      (J,PR/C,73,064609,2006)
#doi:10.1103/PhysRevC.73.064609
FACILITY       (VDG,3INDTAT)
SAMPLE         Target 1.5 mg/cm2 self-supporting foil of 175 Lu
DETECTOR       (SISD)centered at 140 degree
METHOD         (EDE)neutron,proton alpha emission measurement
INC-SOURCE     (POLIS)pulsed 159-MeV 28Si beam from LINAC booster
HISTORY        (20110404C) M.Balasubramaniam,Vijayaraghavan,
Karthikraj,Bharathiar Univ.,Rajeshkumar NIT Hamirpur,
S.Mahadevan Amrita Univ.,S.Subramanian VOC College TN,
G.Pandikumar, IGCAR
COMMENT        Figure 2 measurement at different angles at same
energies
ENDBIB         19          0            D6121  1    22
NOCOMMON      0          0            D6121  1    23
ENDSUBENT     22          0            D6121  199999
SUBENT         D6121002  20110404      D6121  2    1
BIB            2          2            D6121  2    2
REACTION       (71-LU-175(14-SI-28,X)0-NN-1,PR,MLT,NU/DA/DE)
STATUS        (APRVD)
ENDBIB         2          0            D6121  2    5
COMMON        2          3            D6121  2    6
EN            ANG          D6121  2    7
MEV           ADEG         D6121  2    8
159.          105.        D6121  2    9
ENDCOMMON     3          0            D6121  2    10
DATA          2          10           D6121  2    11
  
```

1. Introduction
2. The three cluster model
3. α -accompanied fission of ^{252}Cf
4. Role of deformation and orientation
5. PES of ^{252}Cf in equatorial and collinear configuration
6. Summary

1. Introduction



Superheavy elements are the trans-actinide elements beginning with Rutherfordium ($Z=104$). They have all been made artificially and currently have no practical purpose because of their very short life times from few minutes to few milliseconds making the studies very hard and serve purpose only for research.

The fundamental interest in heavy element research is connected to the questions

How many elements may exist in nature ?

How heavy can nuclei be ?

How do nuclei behave in the presence of strong Coulomb forces?

What would be the next magic numbers for proton and neutron?

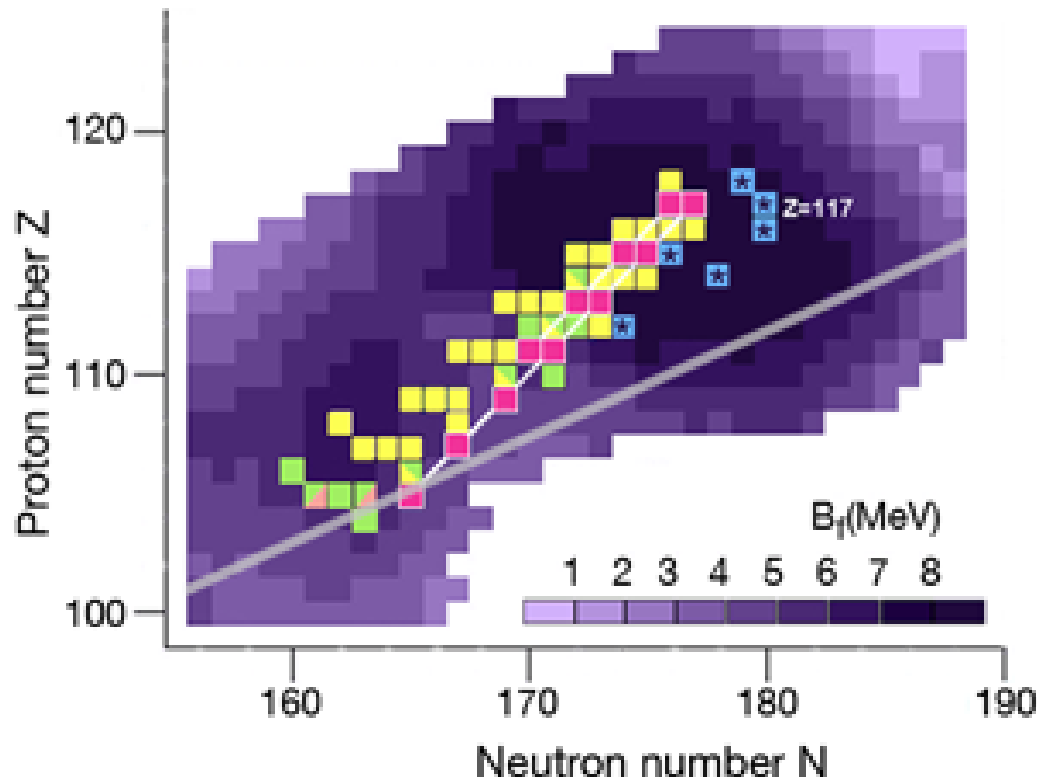
These kind of studies helps as a stringent test to know the validity of existing theoretical models.

- No consensus: (For Island of stability)
- In mid-1960s, a number of theoretical calculations predicted that an atom with the doubly-magic nucleus containing 114 protons and 184 neutrons should be extra stable.
- Different parametrization within the Skyrme HF and RMF produce quite different predictions for the next spherical doubly magic nuclei
- namely $Z = 114, 120$ and/or 126 with $N = 172$ or 184 . (Spherical RMF, Axially deformed RMF, SHF with different parameter sets which reproduces the g.s. properties)
- effective field theory predicts $Z = 120$ and $N = 172$ and $Z = 120$ and $N = 258$ as possible spherical doubly magic superheavy nuclei.

Experimental challenge



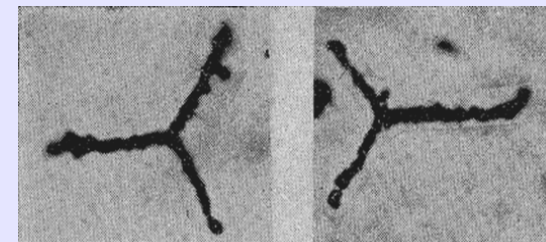
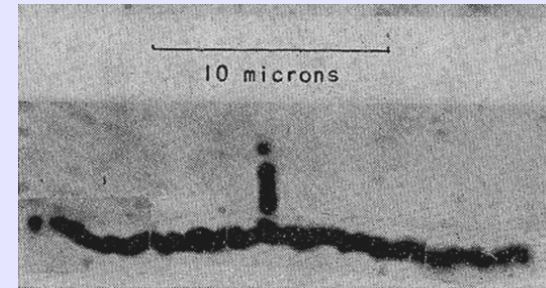
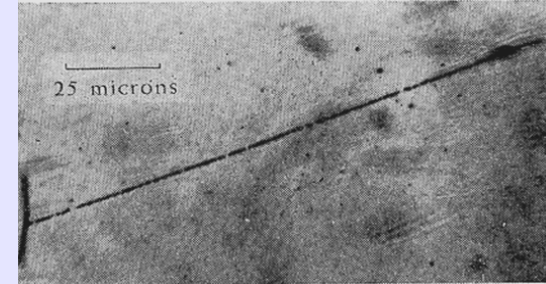
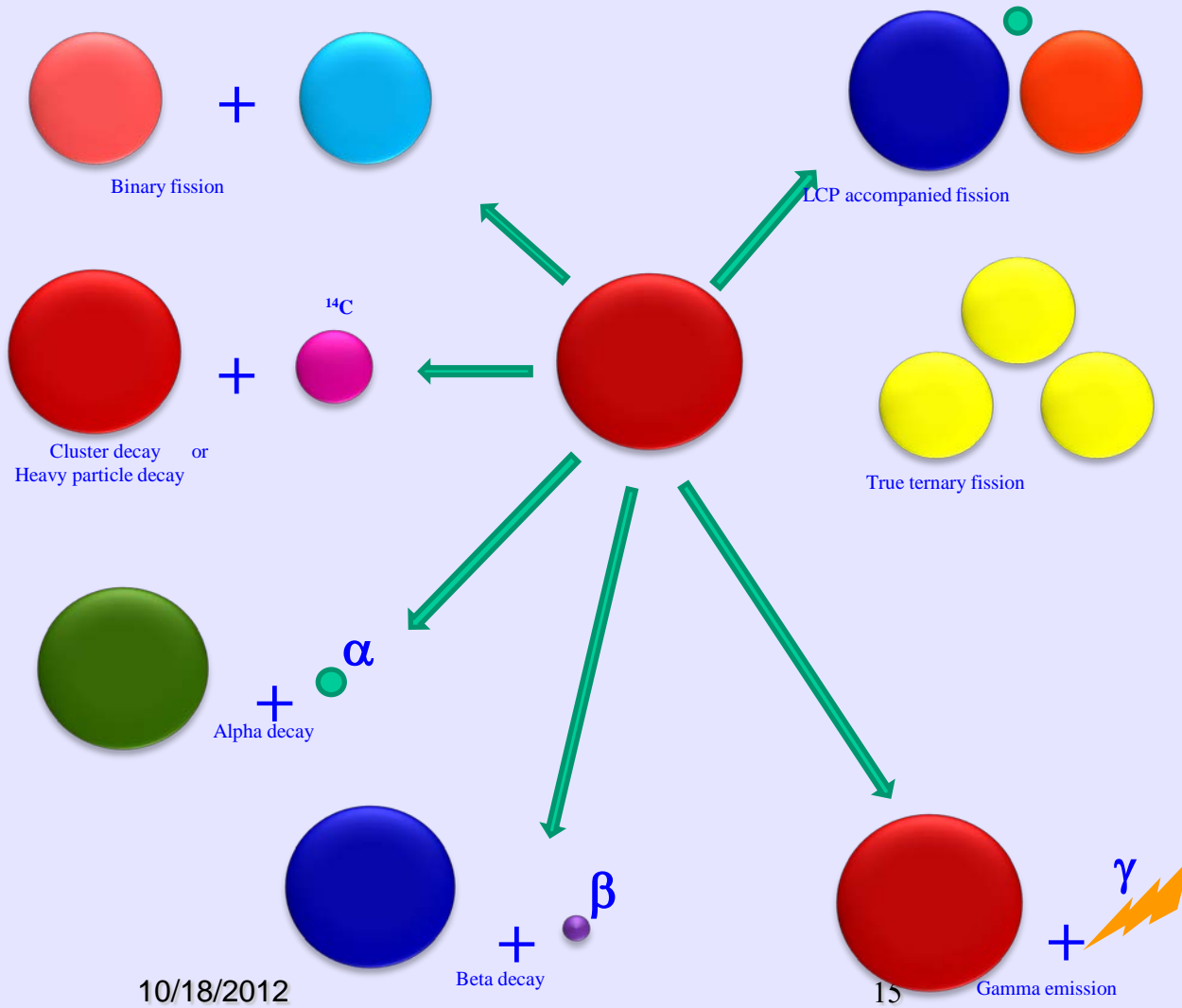
- Over the last thirty years, experimentalists are undergoing an expedition to explore the predicted “island of superheavy elements”—a region of increasingly stable nuclei around atomic number 114
- So far they have reported, on average, the discovery of one new element every two and a half years.



- a new element with atomic number 117. Two isotopes of the new, still unnamed, element were produced from **nuclear fusion reactions** from a beam of ^{48}Ca ions that impinged on target nuclei of ^{249}Bk . (Published in PRL 104(2010)142502). (JINR, RIAR, LLNL, ORNL, VU and UON) – Lead by Yu.Ts. Oganessian
- This was a 2 year campaign began at the High Flux Isotope Reactor in Oak Ridge with a 250-day irradiation to produce 22 mg of berkelium. (3.5 Million dollars, J. Hamilton, A.V. Ramayya of VU)
- followed by 90 days of processing at ORNL to separate and purify the berkelium, target preparation at Dimitrovgrad,
- 150 days of bombardment at most powerful HI accelerators at Dubna
- Data analysis at Livermore and Dubna, and assessment and review of the results by the team.
- This discovery fills the gap between elements 116 and 118, so that now elements are continuously known from $Z=1$ up to element 118



Different decay modes



S. L. Muga *et.al.* (1961)



Hanoipttnew.pdf - Adobe Reader

File Edit View Document Tools Window Help

1 / 26 68.4% Find

True Ternary Fission:

Collinear Cluster Tripartition (CCT)

A new kind of radioactive cluster decay

Wolfram von Oertzen
*Helmholtz-Zentrum BERLIN (former HMI)
and Freie Universität Berlin*

In collaboration with:
Y. V. Pyatkov, D. Kamanin et al. (FLNR, JINR, Dubna)
and M. Balasubramanian (Bharathiar University, Coimbatore, India)

Y.V. Pyatkov, D. Kamanin, W von Oertzen et al., Eur. Phys. J. A •• (2010) 29
K. Manimaran and M. Balasubramanian, Phys.Rev. C•• (2011) 034609

Slide: 1

21:11
05-09-2011



- ❖ Ternary fission is defined as a nuclear break-up into three fragments which covers a spectrum of fission events from one end in which a scission neutron accompanies two main fission fragments, to the other in which three fragments of about equal masses are emitted.
- ❖ The ternary fission process with three charged particles in the outgoing channel, with the third particle being very light compared to the fission fragments are called as particle accompanied fission or light charged particle accompanied fission.
- ❖ The spontaneous break-up into three nuclei of about equal mass the so called true ternary fission has not yet been observed but theoretically is being studied.



First evidence of TF was reported by Alvarez in 1943, $^{235}\text{U}(n, \text{TF})$ with the emission of alpha particles along with main fission fragments.

(Based on LDM in 1958, Swiatecki predicted TF, Quaternary and Quinary Fission)

In TF, the light charged particles are born along with main fragments at **scission configuration**.

The Coulomb force will then expel the light particle roughly at right angles to the heavy fragments motion (also supported by the measured energy spectra and angular distribution.) ($\text{U} \rightarrow \text{Ba} + \text{Kr} + \text{Alpha}$)



This process is a rare one as it occurs about once in ~ 260 binary fission events, in ^{252}Cf .

In TF in some cases the light cluster is also born in an excited state, and decays to ground state by emitting gamma rays.

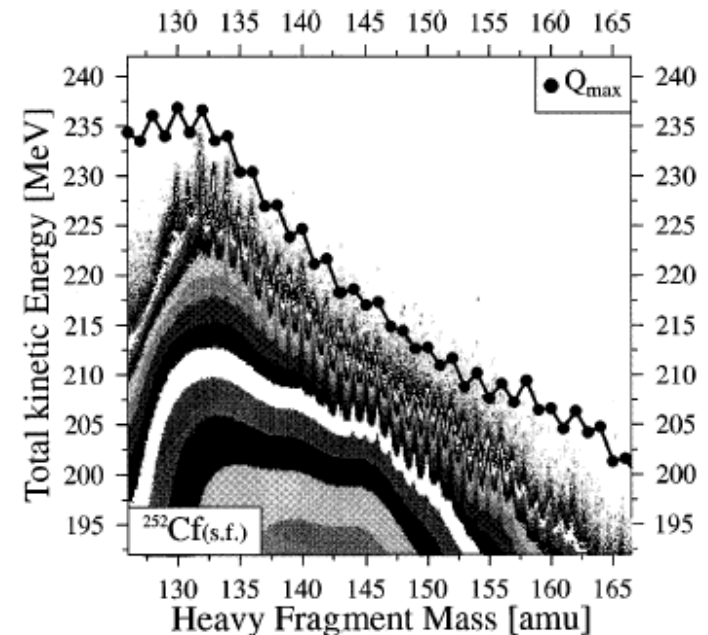
Though a rare process, a major interest has been mounted to obtain additional data to **know more about the dynamics**.

Experiments on TF gives, evidence for two different modes of ternary fission, hot and the cold.

In alpha accompanied fission of ^{252}Cf the majority of the fissions are **hot**, while for ^{10}Be -accompanied fission the **cold process** dominates – as supported by theory

In the limiting case of **cold fission**, the fission process proceeds with no neutron evaporation and in some cases gamma emission is virtually absent, resulting in the formation of fragments into their g.s.

Cold ternary decays should produce all the three fragments at very low excitation energy and, consequently, with very high kinetic energies – very compact shapes at the scission point and deformations close to those of their g.s.



(F. Gonnenwein et al)



LCP	Reaction	Energy (MeV)	MPE (MeV)	Angle
¹ H	²⁵² Cf(sf)	3.3-12	3.5±0.5	91°
¹ H	²⁵² Cf(sf)	3.18-19.62	9±2	-
² H	²⁵² Cf(sf)	3.83-18.22	7±2	-
² H	²⁵² Cf(sf)	4.2-18	-	91°
³ H	²⁵² Cf(sf)	3.89-23.13	8±1	-
³ H	²⁵² Cf(sf)	5-24	-	91°
³ He	²⁵² Cf(sf)	10.75-33.75	17±1	-
⁴ He	²⁵² Cf(sf)	7.75-34.75	16±0.5	-
⁴ He	²⁵² Cf(sf)	9-26	16.0±0.3	-
⁴ He	²⁵² Cf(sf)	7.1-41	-	92°
⁴ He	²⁵² Cf(sf)	-	-	82°
⁴ He	²⁵² Cf(sf)	11-40	15.6±0.2	-
⁴ He	²⁵² Cf(sf)	8-30	15.7±0.2	90°
⁴ He	²⁵² Cf(sf)	9-30	-	-
⁴ He	²⁵² Cf(sf)	0-30	18.0±0.5	-
⁴ He	²⁵² Cf(sf)	12-32	15.6±0.2	-
⁴ He	²⁵¹ Cf(sf)	14-30	16.1±0.1	-
⁴ He	²⁵⁶ Fm(sf)	14.5-31	15.5±0.4	-
⁴ He	²⁵⁷ Fm(sf)	15-35	15.9±0.6	-
⁴ He	²⁴⁴ Pu(sf)	12-40	15.5±0.55	-
⁵ He	²⁵² Cf(sf)	-	12.3±0.9	30-150°
⁵ He	²⁵² Cf(sf)	-	12.4±0.3	-
⁵ He	²⁵² Cf(sf)	11-12	11±0.5	-
⁵ He	²⁵² Cf(sf)	10.75-33.25	13±1	-
⁶ He	²⁵² Cf(sf)	14.6-43	-	93°
⁶ He	²⁵² Cf(sf)	10-22	12.3±0.5	90°
⁸ He	²⁵² Cf(sf)	12-36	≤13	-
⁸ He	²⁵² Cf(sf)	9.6-46	-	-
Li	²⁵² Cf(sf)	19-39	-	-
Li	²⁵² Cf(sf)	15.7-65	-	-
Li	²⁵² Cf(sf)	17-35	14.3±10	84.9°
Be	²⁵² Cf(sf)	33-41	-	-
¹⁰ Be	²⁵² Cf(sf)	24-73	-	-
¹⁰ Be	²⁵² Cf(sf)	18.8±0.4	-	-
B	²⁵² Cf(sf)	-	20.5±1	-
B	²⁵² Cf(sf)	25-50	26±0.5	-
C	²⁵² Cf(sf)	32-34	-	-
¹⁴ C	²⁵² Cf(sf)	30-50	34±0.5	-

LCP	Reaction	Energy (MeV)	MPE (MeV)	Yield
³ H	²³⁵ U(n, f)	-	8.0±0.2	-
³ H	²³⁵ U(n, f)	5-18	15.8±0.1	-
³ H	²³⁵ U(n, f)	5-18	15.8±0.1	-
³ H	²³⁹ Pu(n, f)	5-18	15.9±0.2	-
³ H	²⁴¹ Pu(n, f)	5-18	15.9±0.3	-
⁴ He	²³⁵ U(n, f)	10-34	15.8±0.1	-
⁴ He	²³⁵ U(n, f)	8-26	15.4±0.2	-
⁴ He	²³⁵ U(n, f)	10-32	15.8±0.1	-
⁴ He	²³⁹ Pu(n, f)	8-34	15.9±0.1	-
⁴ He	²⁴¹ Pu(n, f)	10-35	15.9±0.1	-
⁴ He	²⁵² Th(n, f)	8-28	15.8±0.2	-
⁵ He	²³⁵ U(n, f)	11	11.6±1.4	-
⁸ Li	²⁴⁹ Cf(n, f)	-	15.1±1.4	2.6±0.7×10 ⁻⁶
⁹ Li	²⁴⁹ Cf(n, f)	-	12.5±0.9	3.8±1.6×10 ⁻⁶
¹⁰ Be	²⁴⁹ Cf(n, f)	-	17.5±0.4	3.8±0.7×10 ⁻⁶
¹¹ Be	²⁴⁹ Cf(n, f)	-	16.5±1.3	4.7±1.2×10 ⁻⁶
¹² Be	²⁴⁹ Cf(n, f)	-	15.1±1.1	2.7±0.7×10 ⁻⁶
¹² Be	²⁴⁹ Cf(n, f)	-	21.8±0.3	1.5±0.4×10 ⁻⁶
¹³ B	²⁴⁹ Cf(n, f)	-	20.1±1.1	2.4±0.6×10 ⁻⁶
¹⁴ B	²⁴⁹ Cf(n, f)	-	17.0±1.2	1.4±0.4×10 ⁻⁶
¹⁵ B	²⁴⁹ Cf(n, f)	-	16.8±1.9	9.1±4.1×10 ⁻⁶
¹⁴ C	²⁴⁹ Cf(n, f)	-	27.6±0.3	1.3±0.2×10 ⁻⁶
¹⁵ C	²⁴⁹ Cf(n, f)	-	25.1±0.5	5.3±1.1×10 ⁻⁶
¹⁶ C	²⁴⁹ Cf(n, f)	-	24.4±1.1	4.8±1.1×10 ⁻⁶
¹⁷ C	²⁴⁹ Cf(n, f)	-	21.3±1.7	7.5±2.8×10 ⁻⁷
¹⁸ C	²⁴⁹ Cf(n, f)	-	20.4±2.8	2.4±0.7×10 ⁻⁷
¹⁶ N	²⁴⁹ Cf(n, f)	-	25.9±2.2	1.5±0.4×10 ⁻⁷
¹⁷ N	²⁴⁹ Cf(n, f)	-	25.0±1.6	8.1±2.0×10 ⁻⁷
¹⁸ N	²⁴⁹ Cf(n, f)	-	23.8±1.5	4.5±1.1×10 ⁻⁷
²⁰ O	²⁴⁹ Cf(n, f)	-	31.4±1.7	25.0±0.7×10 ⁻⁶
²¹ O	²⁴⁹ Cf(n, f)	-	24.2±1.2	6.4±1.3×10 ⁻⁷
²² O	²⁴⁹ Cf(n, f)	-	33.0±7.4	4.2±1.6×10 ⁻⁷
²¹ F	²⁴⁹ Cf(n, f)	-	26.0±2.1	1.6±0.4×10 ⁻⁷
²² F	²⁴⁹ Cf(n, f)	-	33.8±10.5	1.4±0.8×10 ⁻⁷
²⁴ F	²⁴⁹ Cf(n, f)	-	26.3±2.8	8.3±4.0×10 ⁻⁸
²⁴ Ne	²⁴⁹ Cf(n, f)	-	33.9±2.9	2.4±0.6×10 ⁻⁷
²⁷ Na	²⁴⁹ Cf(n, f)	-	38.4±8.2	8.2±3.2×10 ⁻⁸
³⁰ Na	²⁴⁹ Cf(n, f)	-	31.7±8.6	2.2±2.2×10 ⁻⁸
³⁰ Mg	²⁴⁹ Cf(n, f)	-	34.9±3.7	1.3±0.4×10 ⁻⁷

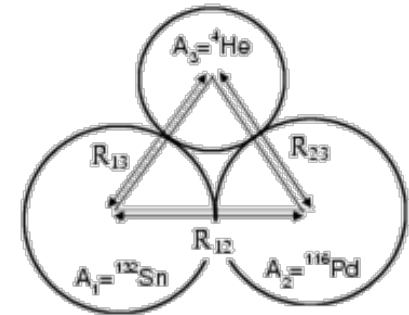
2. Three Cluster Model



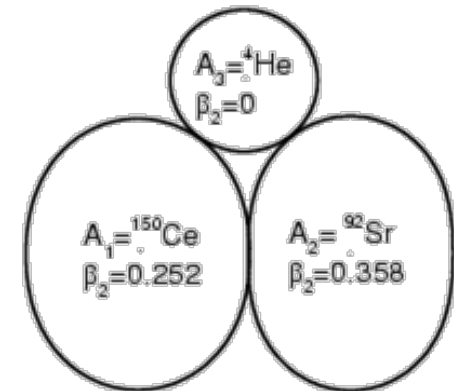
Three cluster model is worked out in terms of:

- I. Mass asymmetry (η)
- II. Charge asymmetry (η_z)
- III. Relative separation (R)
- IV. Deformation (β_2)
- V. Orientation angle (θ)
- VI. Fragment mass number (A_3)

a) Spherical



b) With $\beta_2, 90^\circ - 90^\circ$



$$\eta = \frac{A_1 - A_2}{A_1 + A_2}$$

$$\eta_z = \frac{Z_1 - Z_2}{Z_1 + Z_2}$$



$Q = E_1 + E_2 + E_3$ with Q -value for the three decay products defined as

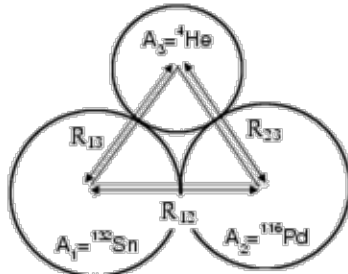
$$Q = M - \sum_{i=1}^3 m_i$$

M – Mass excess of decaying nucleus
 m – mass excesses of product nuclei.

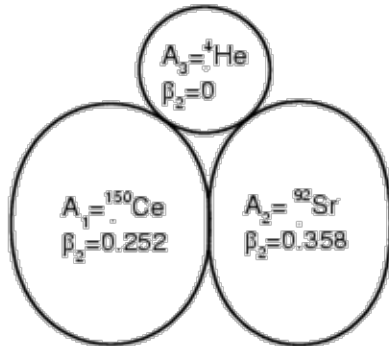
The three body ternary fragmentation potential is defined as

$$V_{tot} = \sum_{i=1}^3 \sum_{j>i}^3 (B_{ii} + V_{ij}) \left. \vphantom{\sum_{i=1}^3 \sum_{j>i}^3} \right\} \begin{array}{l} B_{ii} \text{ are binding energies} \\ V_{ij} = V_{Cij} + V_{Nij} \end{array}$$

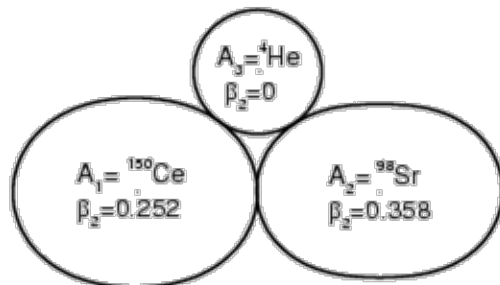
a) Spherical



b) With $\beta_2, 90^\circ - 90^\circ$



c) With $\beta_2, 0^\circ - 0^\circ$



10/18/2012

The Coulomb interaction between the three spherical nuclei is given as

$$V_{Cij} = \frac{Z_i Z_j e^2}{R_{ij}^s}$$

For deformed and oriented case

$$V_C = \sum_{i,j} \frac{Z_i Z_j e^2}{R_{ij}^s} + 3Z_i Z_j e^2 \times \sum_{\lambda, k=i,j} \frac{1}{2\lambda+1} \frac{R_k^\lambda(\alpha_k)}{R^{\lambda+1}} Y_\lambda^{(0)}(\theta_k) \times \left[\beta_{\lambda k} + \frac{4}{7} \beta_{\lambda k}^2 Y_\lambda^{(0)}(\theta_k) \right]$$



With,

$$R_{ij}^s = R_{ij} + S_{ij}$$

$$R_{ij} = r_0 \left(A_i^{1/3} + A_j^{1/3} \right)$$

the relative separation
between fragments,

Radius of the fragments

$$R_{0i} = 1.28A_i^{1/3} - 0.76 + 0.8A_i^{-1/3}$$

Spherical case

$$R_i(\alpha_i) = R_{0i} \left[1 + \sum_{\lambda} \beta_{\lambda i} Y_{\lambda}^{(0)}(\alpha_i) \right]$$

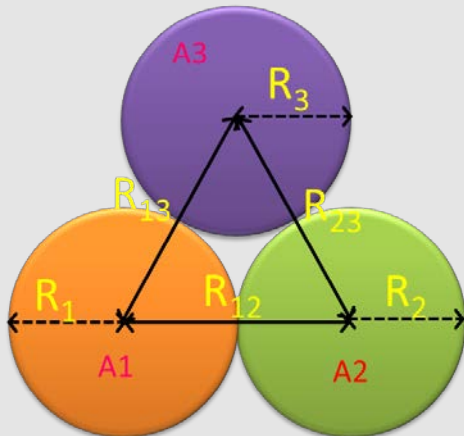
Deformed case



S_{ij} - surface separation

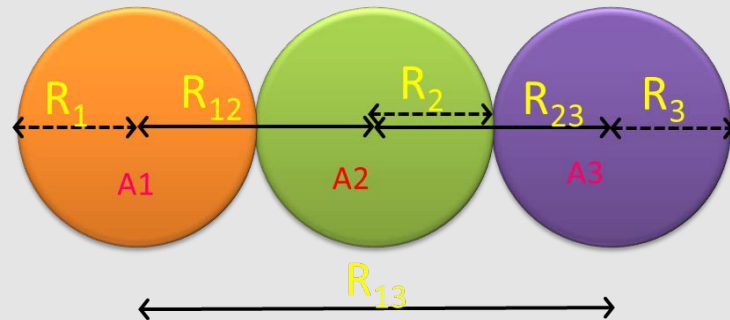
For touching configuration, $s = s_{12} = s_{13} = s_{23} = 0$

Equatorial configuration



$$s_{12} = s_{23} = s_{13} = s$$

Collinear configuration



$$s_{12} = s_{23} = s; \quad s_{13} = 2(R_2 + s)$$



For attractive part

Nuclear interaction potential (V_{Nij})

Yukawa plus exponential potential (For spherical fragments)

$$V_{Nij} = -4 \left(\frac{a}{r_0} \right)^2 \sqrt{a_{2i} a_{2j}} \times \left[g_i g_j \left(4 + \frac{R_{ij}}{a} \right) - g_j f_i - g_i f_j \right] \frac{\exp \left(- \frac{R_{ij}}{a} \right)}{R_{ij}/a}$$

Nuclear Proximity potential (For deformed fragments)

$$V_P = 4\pi \bar{R} \gamma b \phi(\xi)$$



In TCM the decay constant and half-life are defined as

$$\lambda = PP_0P_3\nu; \quad T_{1/2} = \frac{\ln 2}{\lambda}$$

$\nu \rightarrow$ is the assault frequency

$P_3 \rightarrow$ is the preformation probability of the third fragment (assumed to be equal to unity)

$P_0 \rightarrow$ is the preformation probability of the other two fragments calculated by solving Schrodinger equation

$P \rightarrow$ is the penetration probability of the fragments to cross the interaction barrier

$$P = \exp \left[-\frac{2}{\hbar} \int_{s_1}^{s_2} \{2\mu[V(s) - Q]\}^{1/2} ds \right]$$

The relative yield for all the charge minimized ternary fragmentation channels are calculated

$$Y(A_i, Z_i) = \frac{P(A_i, Z_i)}{\sum P(A_i, Z_i)}$$

3. α -accompanied fission of ^{252}Cf

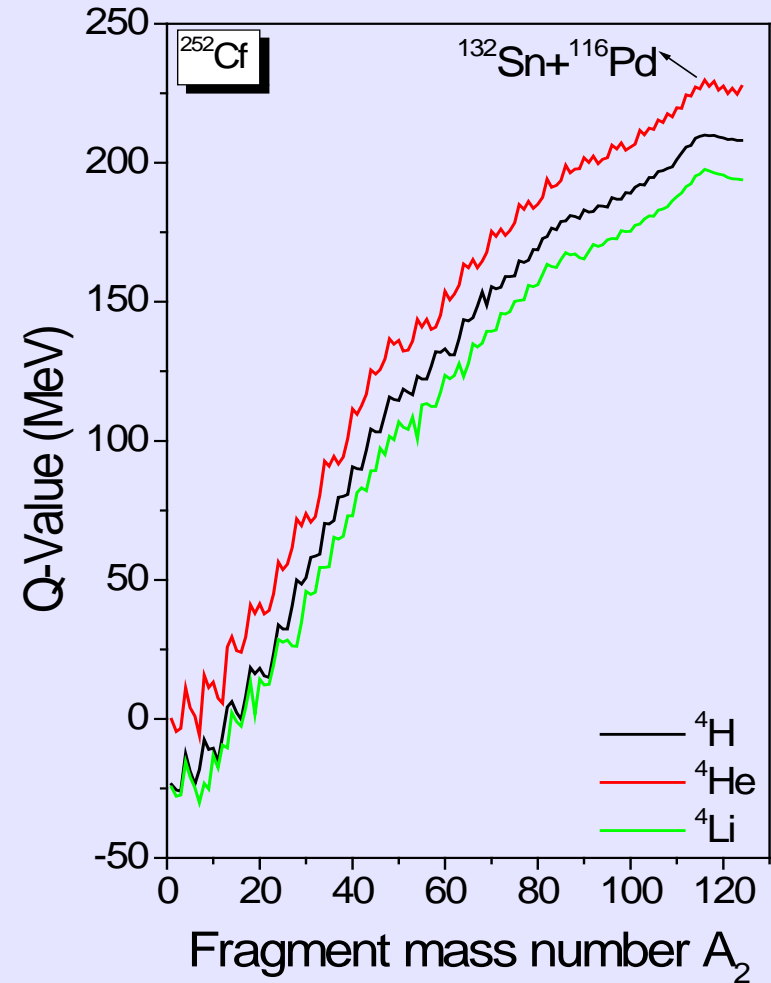
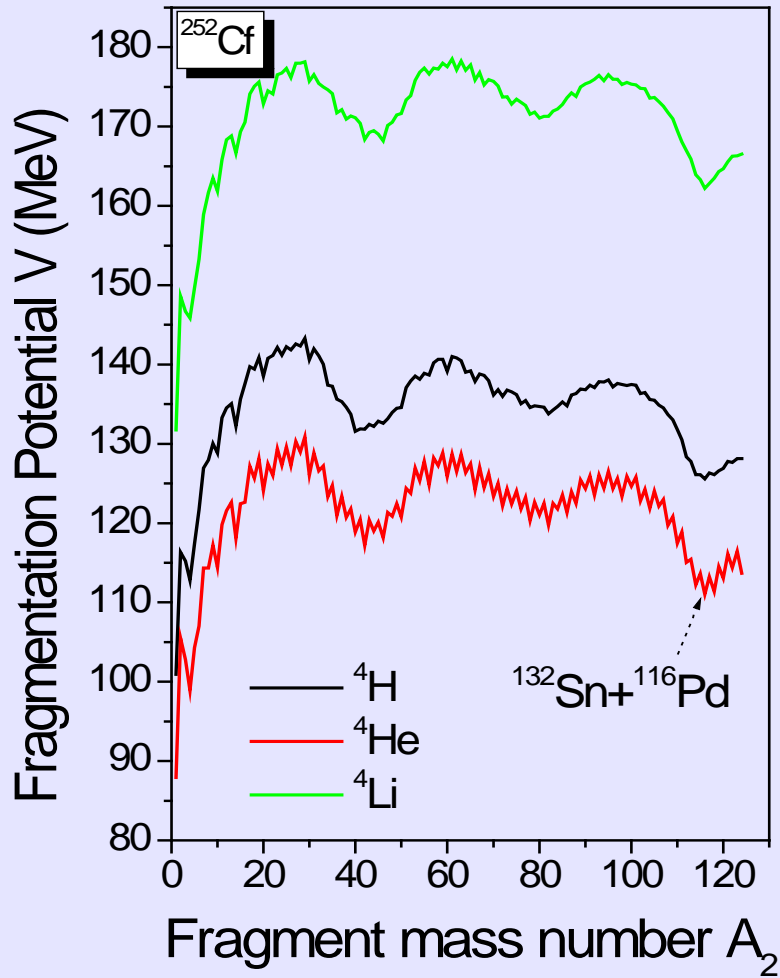


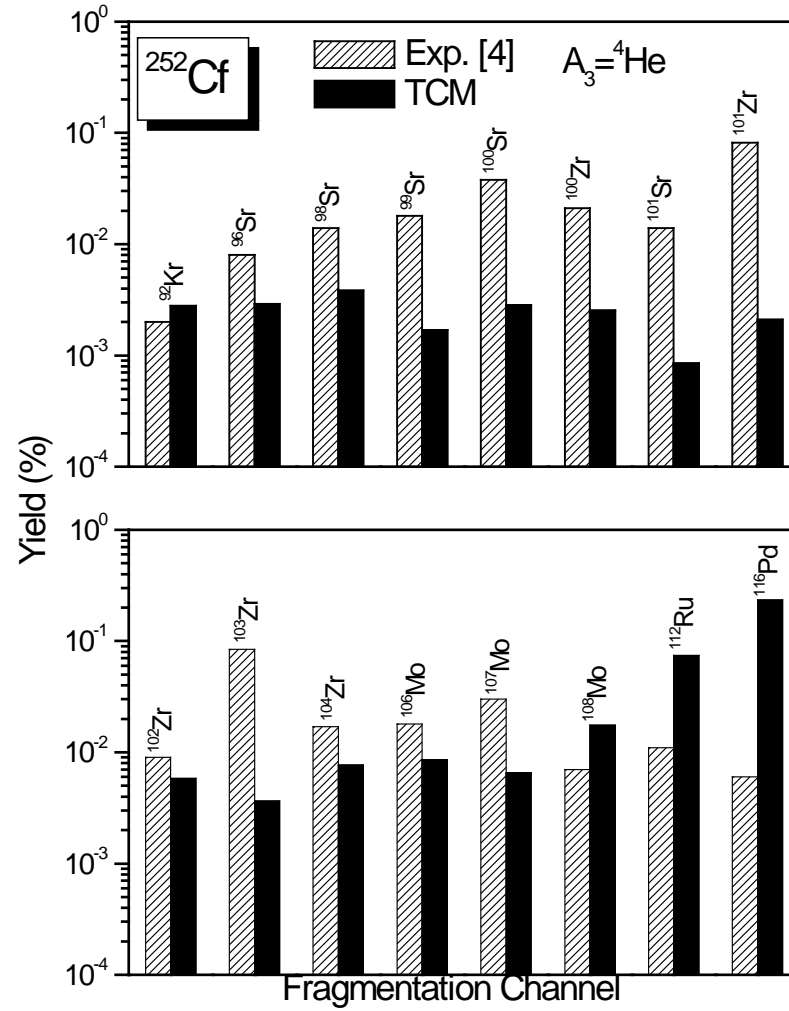
Californium (Cf) nuclei offer interesting possibilities for both the theoretical and experimental investigations of various spontaneous decay modes such as Spontaneous binary fission, ternary fission and cluster radioactivity.

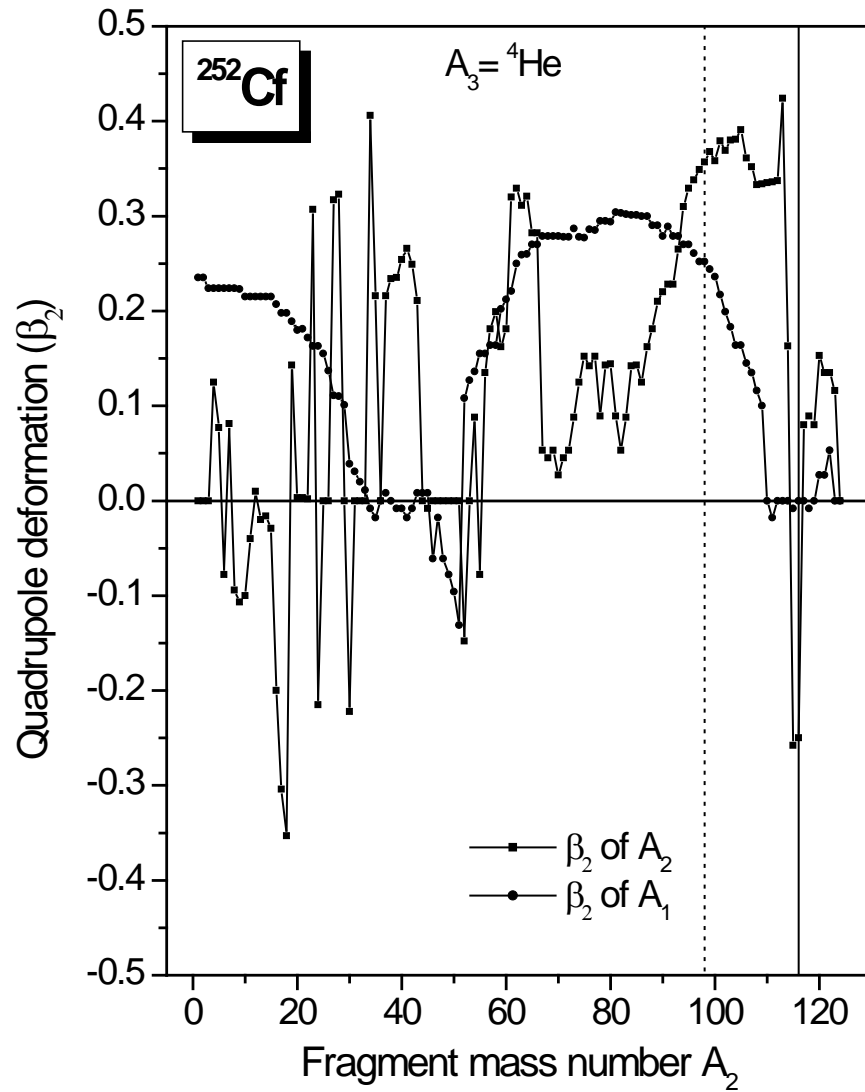
Spontaneous ternary fissions of ^{252}Cf have been recently studied quite extensively with ^4He , ^{10}Be and ^{14}C nuclei as third particle.

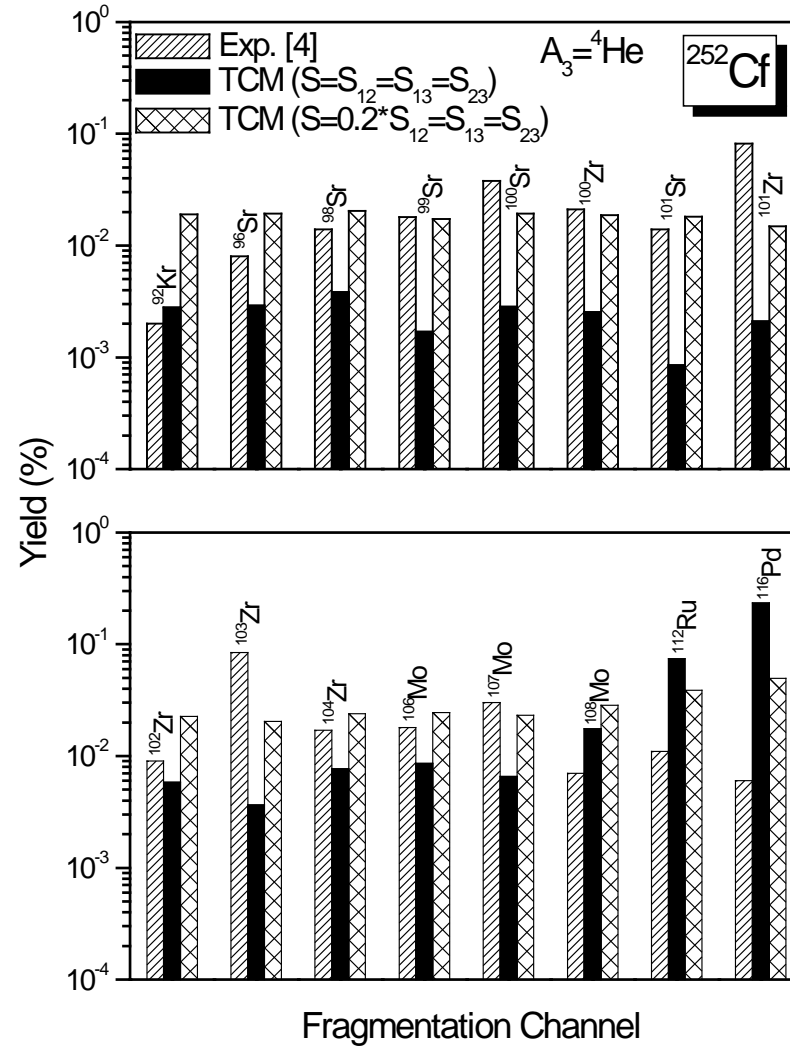
The cold α -accompanied TF of ^{252}Cf was recently observed by Ramayya *et al* in which the yields for correlated pair of **Kr-Nd**, **Sr-Ce**, **Zr-Ba**, **Mo-Xe**, **Ru-Te**, **Pd-Sn** associated with ^4He as the third particle has been measured.

This experiment was the first evidence for the cold (neutron less) ternary fission.









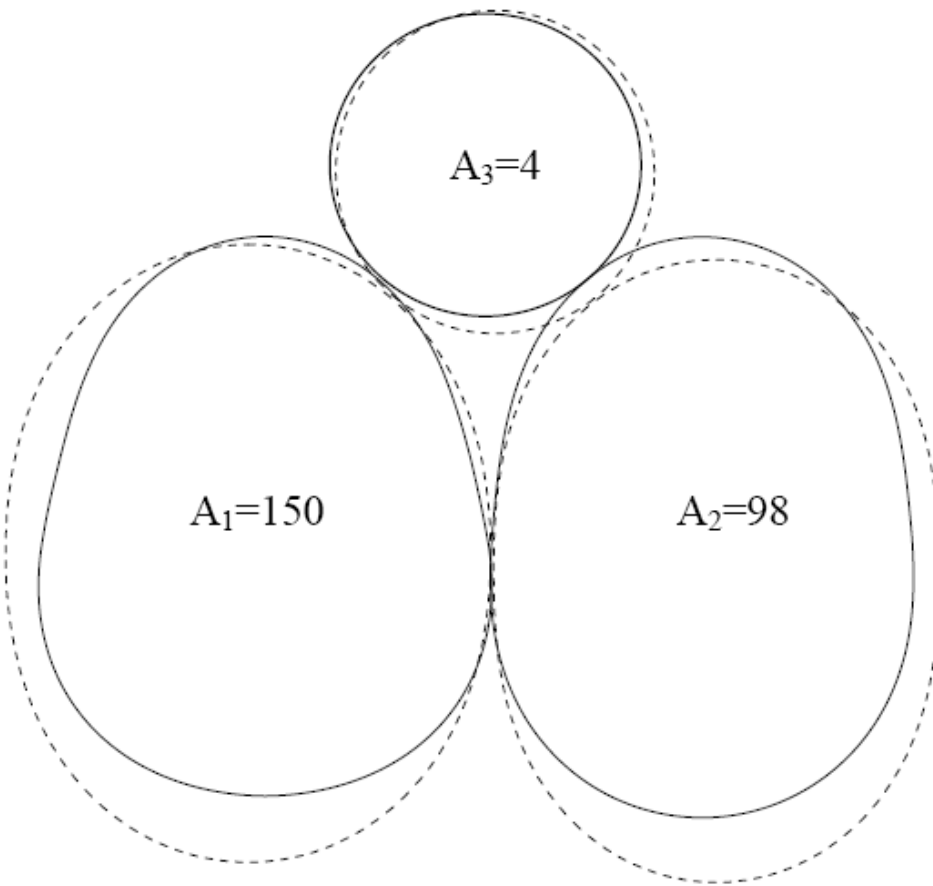
4. Role of deformation and orientation



In TCM, we are considering the heavy (A_1) and light (A_2) fragments as deformed (and the LCP (A_3) as spherical). Their interaction potentials are calculated by including these effects.

With incorporation of deformation,

we studied 90-90 (Belly-Belly) and 0-0 (Pole-Pole) orientations.



Belly – Belly

$90^\circ-90^\circ$

Dashed line - β_2

Solidline - $\beta_2+\beta_4$

$A_1=^{150}\text{Ce}$ $A_2=^{98}\text{Sr}$

Pole – Pole

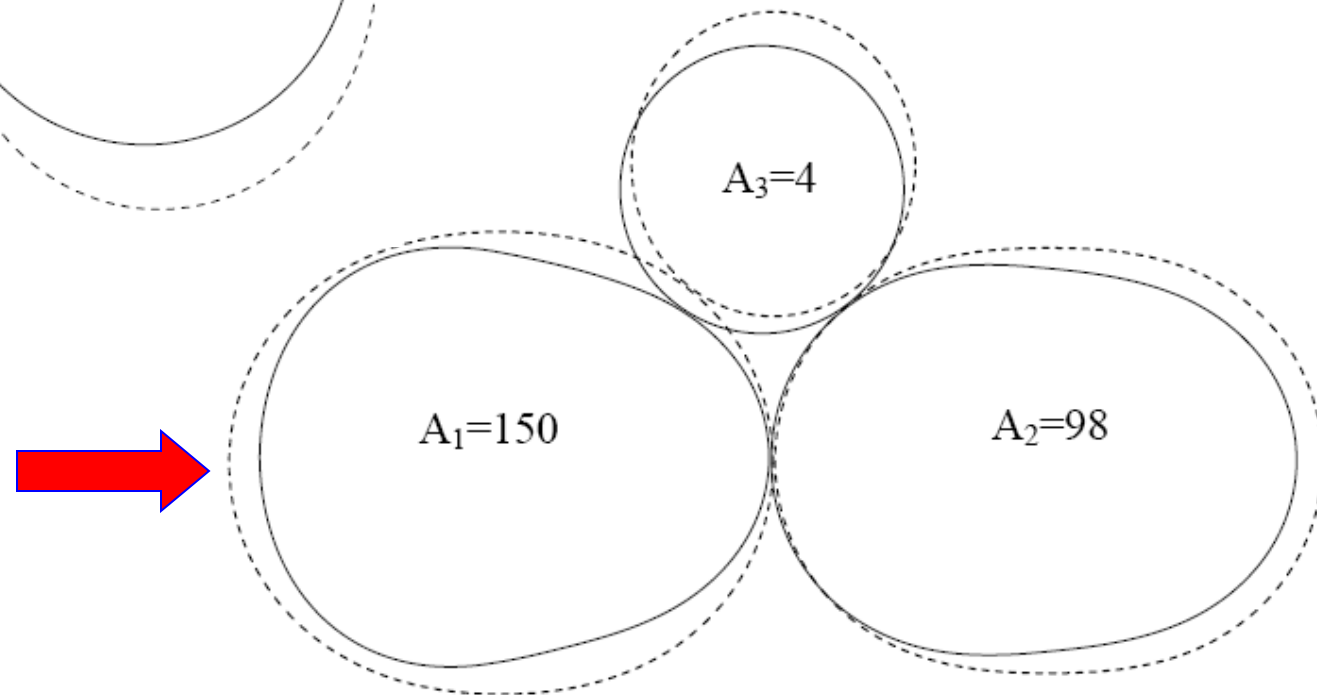
$0^\circ-0^\circ$

Dashed line - β_2

Solidline - $\beta_2+\beta_4$

$A_1=^{150}\text{Ce}$ $A_2=^{98}\text{Sr}$

10/18/2012

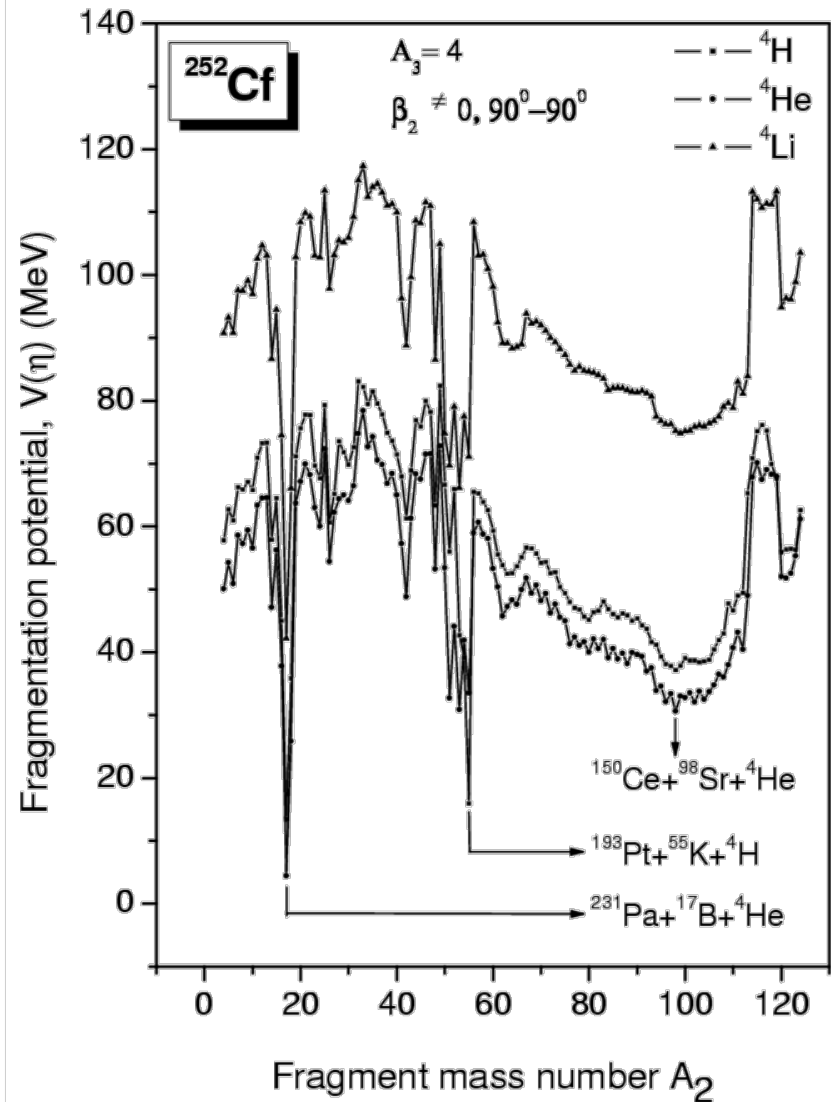
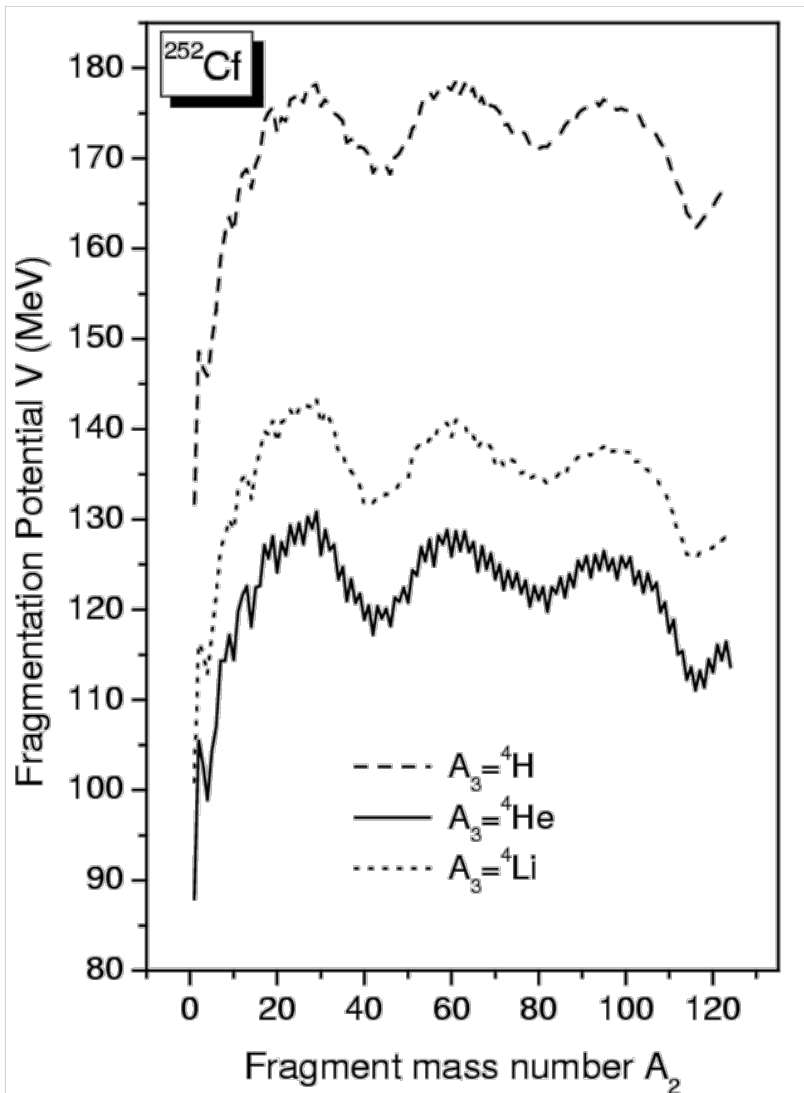


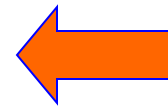
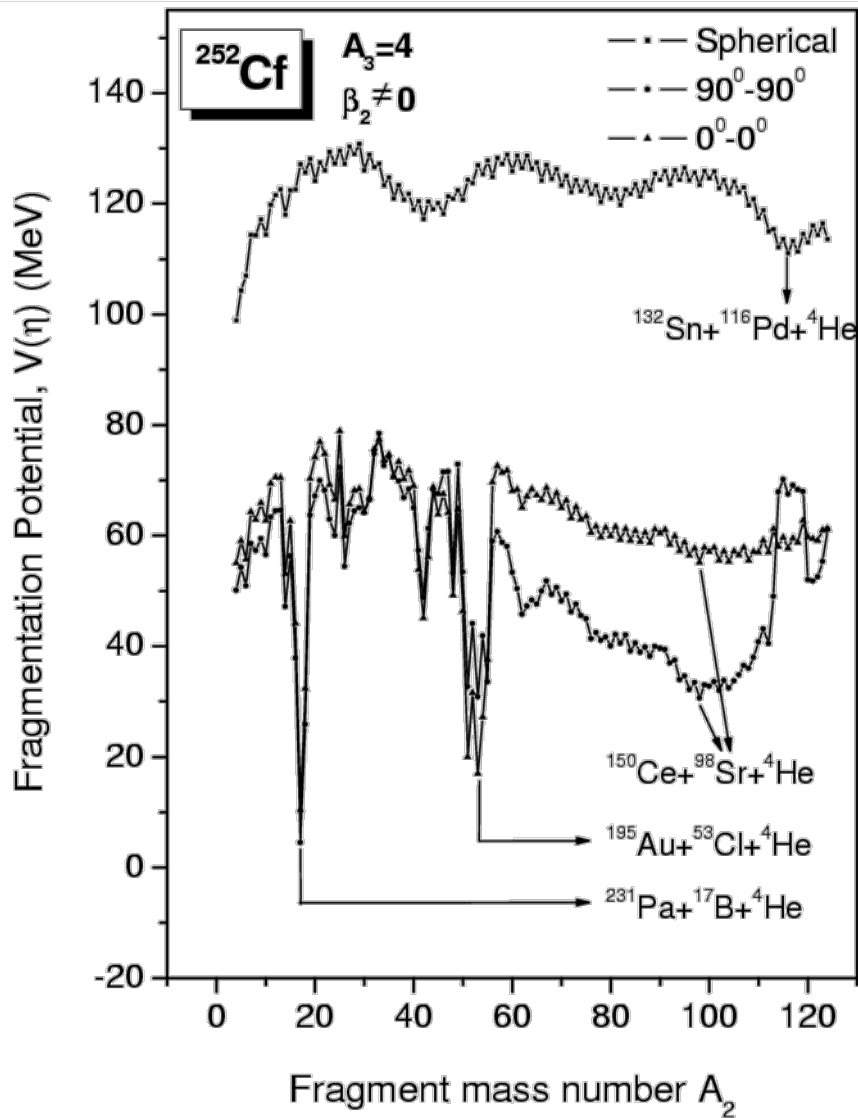


For Spherical case the deep minima in PES - Sn+ Pd+
He (^4He accompanied TF of ^{252}Cf)

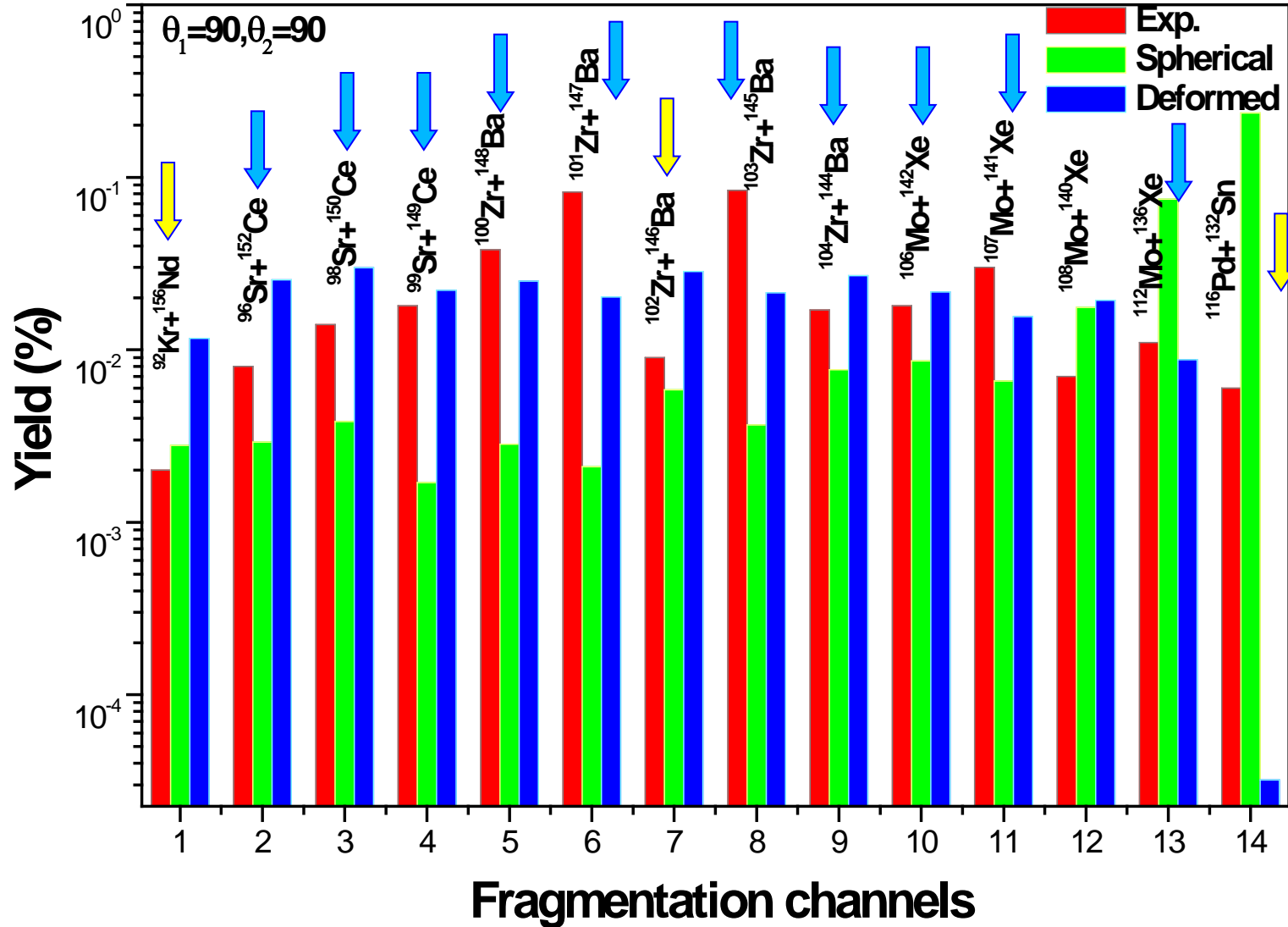
The experimentally measured yields, has largest yields
for the fragment combinations like Zr-Ba, Sr-Ce.

With deformation and orientation included the minima
in spherical case were no longer present rather new cold
valleys are seen in the PES.





$90^\circ-90^\circ$ is the
Minimum
Among all

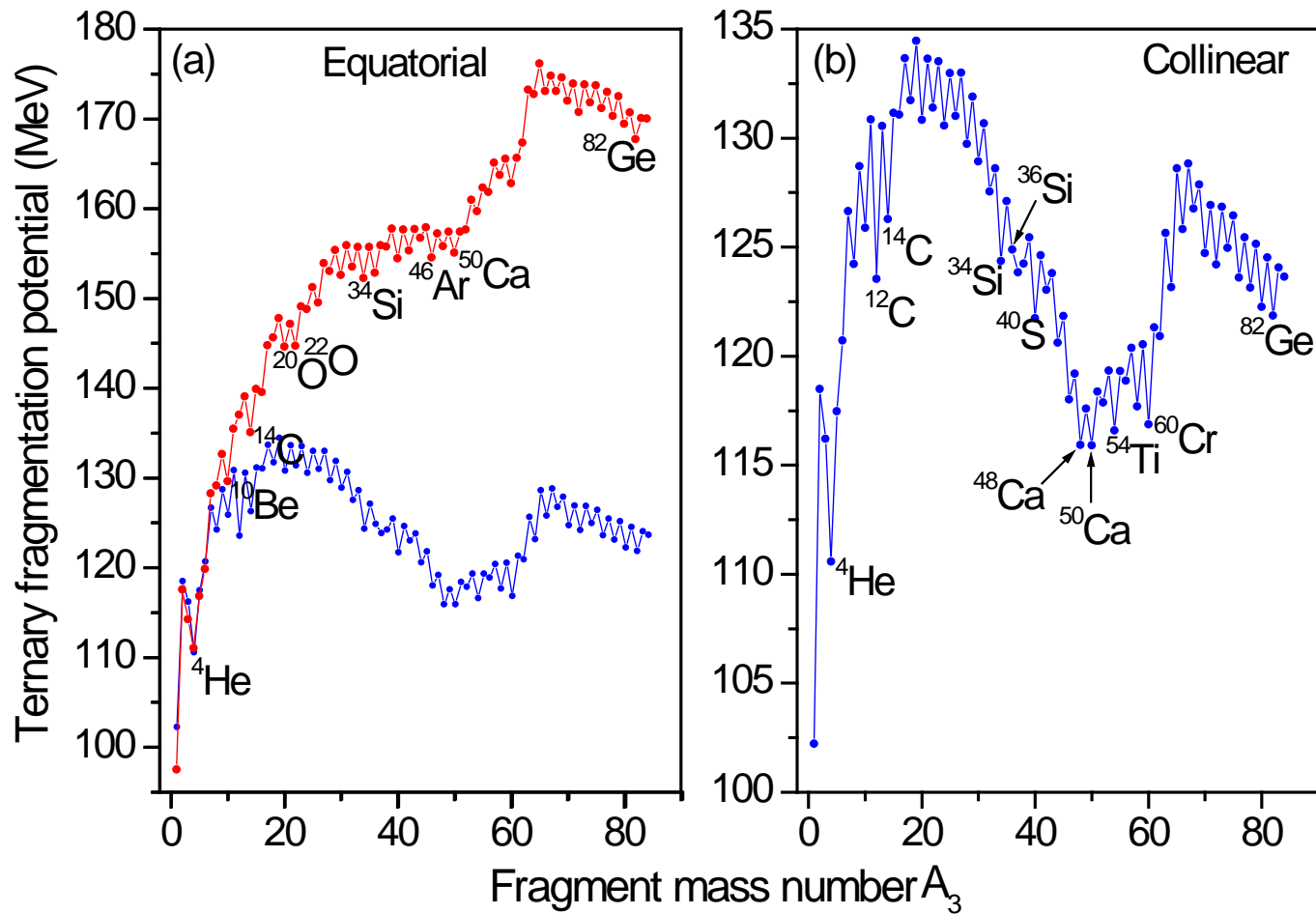




These results clearly shows that, the inclusion of deformation indeed increases the yield values favourable to the experimental values and in particular corresponding to 90-90 orientation matches well with that of experimental results.



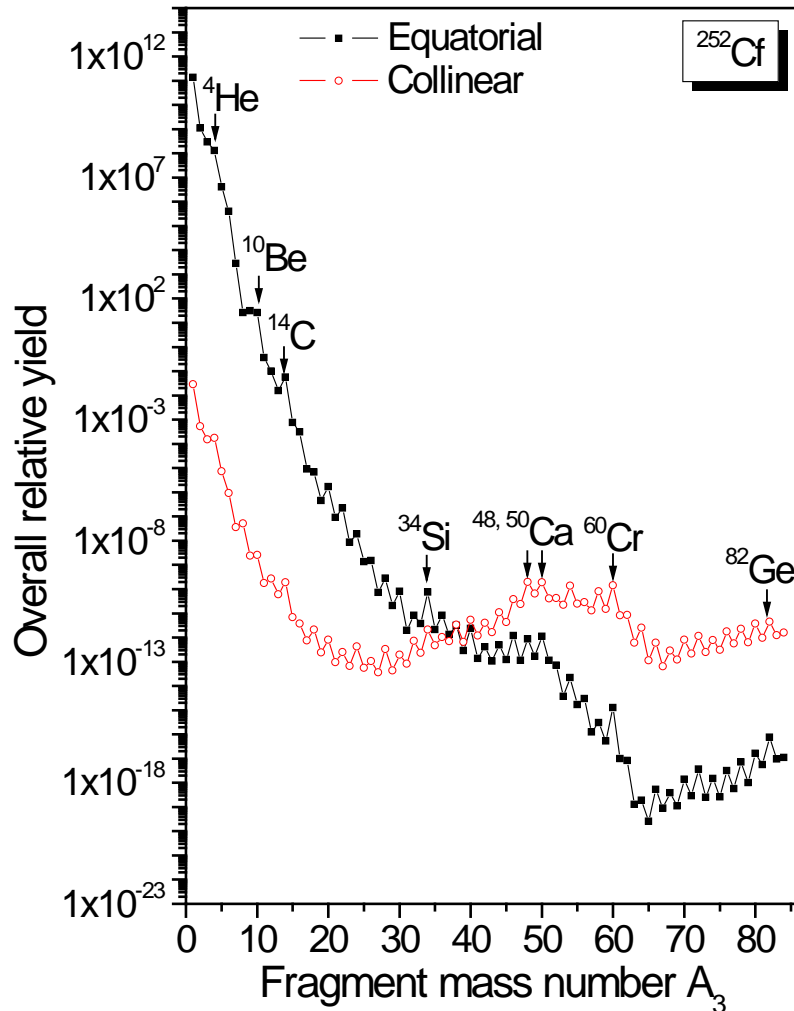
- ❖ If a system A undergoes ternary fission it can have thousands possibilities with respect mass asymmetries and charge asymmetries.
- ❖ To avoid the repetition of fragmentation
$$A_1 \geq A_2 \geq A_3$$
- ❖ All the possible ternary fragmentations of ^{252}Cf in two different configurations (Equatorial and Collinear) are studied
- ❖ The third fragment can have mass number $A_3 = 1$ to 84.





Equatorial configuration			Collinear configuration		
Fragmentation channel	V(η) (MeV)	Q value (MeV)	Fragmentation channel	V(η) (MeV)	Q value (MeV)
$^{130}\text{Sn}+^{121}\text{Cd}+^1\text{n}$	97.51	229.36	$^{130}\text{Sn}+^{121}\text{Cd}+^1\text{n}$	102.23	229.36
$^{131}\text{Sn}+^{119}\text{Ag}+^2\text{H}$	117.59	218.76	$^{131}\text{Sn}+^{119}\text{Ag}+^2\text{H}$	118.49	218.76
$^{133}\text{Sb}+^{116}\text{Pd}+^3\text{H}$	114.26	219.80	$^{133}\text{Sb}+^{116}\text{Pd}+^3\text{H}$	116.20	219.80
$^{132}\text{Sn}+^{116}\text{Pd}+^4\text{He}$	111.05	229.76	$^{132}\text{Sn}+^{116}\text{Pd}+^4\text{He}$	110.58	229.76
$^{131}\text{Sn}+^{116}\text{Pd}+^5\text{He}$	116.82	221.95	$^{131}\text{Sn}+^{116}\text{Pd}+^5\text{He}$	117.47	221.95
$^{130}\text{Sn}+^{116}\text{Pd}+^6\text{He}$	119.85	218.73	$^{130}\text{Sn}+^{116}\text{Pd}+^6\text{He}$	120.71	218.73
$^{133}\text{Sb}+^{112}\text{Ru}+^7\text{Li}$	128.28	215.44	$^{133}\text{Sb}+^{112}\text{Ru}+^7\text{Li}$	126.65	215.44
$^{132}\text{Sn}+^{112}\text{Ru}+^8\text{Be}$	129.16	222.85	$^{132}\text{Sn}+^{112}\text{Ru}+^8\text{Be}$	124.22	222.85
$^{131}\text{Sn}+^{112}\text{Ru}+^9\text{Be}$	132.68	217.59	$^{131}\text{Sn}+^{112}\text{Ru}+^9\text{Be}$	128.70	217.59
$^{134}\text{Te}+^{106}\text{Mo}+^{10}\text{Be}$	129.67	218.00	$^{134}\text{Te}+^{106}\text{Mo}+^{10}\text{Be}$	125.88	218.00
$^{134}\text{Te}+^{107}\text{Mo}+^{11}\text{Be}$	135.48	212.01	$^{133}\text{Sb}+^{108}\text{Mo}+^{11}\text{B}$	130.85	217.61
$^{134}\text{Te}+^{108}\text{Mo}+^{12}\text{Be}$	137.01	210.77	$^{132}\text{Sn}+^{108}\text{Mo}+^{12}\text{C}$	123.54	223.72
$^{133}\text{Sb}+^{108}\text{Mo}+^{13}\text{B}$	139.07	214.96	$^{132}\text{Sn}+^{107}\text{Mo}+^{13}\text{C}$	130.54	222.17
$^{132}\text{Sn}+^{108}\text{Mo}+^{14}\text{C}$	135.08	225.94	$^{134}\text{Te}+^{104}\text{Zr}+^{14}\text{C}$	126.28	223.20
$^{134}\text{Te}+^{108}\text{Zr}+^{15}\text{C}$	139.90	218.27	$^{134}\text{Te}+^{108}\text{Zr}+^{15}\text{C}$	131.15	216.90
$^{134}\text{Te}+^{102}\text{Zr}+^{16}\text{C}$	139.55	218.46	$^{134}\text{Te}+^{102}\text{Zr}+^{16}\text{C}$	131.07	218.46
$^{133}\text{Sb}+^{102}\text{Zr}+^{17}\text{N}$	144.78	219.96	$^{133}\text{Sb}+^{102}\text{Zr}+^{17}\text{N}$	133.66	219.96
$^{132}\text{Sn}+^{102}\text{Zr}+^{18}\text{O}$	145.64	226.05	$^{132}\text{Sn}+^{102}\text{Zr}+^{18}\text{O}$	131.74	226.05
$^{132}\text{Sn}+^{101}\text{Zr}+^{19}\text{O}$	147.79	216.67	$^{131}\text{Sn}+^{102}\text{Zr}+^{19}\text{O}$	134.45	223.08
$^{132}\text{Sn}+^{100}\text{Zr}+^{20}\text{O}$	144.61	226.17	$^{134}\text{Te}+^{98}\text{Sr}+^{20}\text{O}$	130.83	223.24
$^{134}\text{Te}+^{100}\text{Zr}+^{21}\text{O}$	147.18	220.58	$^{134}\text{Te}+^{97}\text{Sr}+^{21}\text{O}$	133.63	220.58
$^{134}\text{Te}+^{96}\text{Sr}+^{22}\text{O}$	144.74	223.05	$^{134}\text{Te}+^{96}\text{Sr}+^{22}\text{O}$	131.39	223.05
$^{134}\text{Te}+^{95}\text{Sr}+^{23}\text{O}$	149.10	218.90	$^{133}\text{Sb}+^{96}\text{Sr}+^{23}\text{F}$	133.52	224.68
$^{132}\text{Sn}+^{96}\text{Sr}+^{24}\text{Ne}$	148.79	231.40	$^{132}\text{Sn}+^{96}\text{Sr}+^{24}\text{Ne}$	130.58	231.40
$^{131}\text{Sn}+^{96}\text{Sr}+^{25}\text{Ne}$	151.25	228.66	$^{134}\text{Te}+^{98}\text{Kr}+^{26}\text{Ne}$	132.98	224.72
$^{134}\text{Te}+^{92}\text{Kr}+^{26}\text{Ne}$	149.55	226.85	$^{134}\text{Te}+^{92}\text{Kr}+^{26}\text{Ne}$	131.02	226.85
$^{133}\text{Sb}+^{92}\text{Kr}+^{27}\text{Na}$	153.92	228.53	$^{133}\text{Sb}+^{92}\text{Kr}+^{27}\text{Na}$	133.00	228.53
$^{132}\text{Sn}+^{92}\text{Kr}+^{28}\text{Mg}$	153.04	235.41	$^{132}\text{Sn}+^{92}\text{Kr}+^{28}\text{Mg}$	129.73	235.41
$^{132}\text{Sn}+^{91}\text{Kr}+^{29}\text{Mg}$	155.40	232.71	$^{135}\text{Te}+^{88}\text{Se}+^{29}\text{Mg}$	131.90	228.49
$^{134}\text{Te}+^{88}\text{Se}+^{30}\text{Mg}$	152.60	231.38	$^{134}\text{Te}+^{88}\text{Se}+^{30}\text{Mg}$	128.92	231.38
$^{135}\text{Te}+^{86}\text{Se}+^{31}\text{Mg}$	155.90	228.05	$^{133}\text{Sb}+^{88}\text{Se}+^{31}\text{Mg}$	130.68	226.27
$^{134}\text{Te}+^{86}\text{Se}+^{32}\text{Mg}$	153.54	230.30	$^{132}\text{Sn}+^{88}\text{Se}+^{32}\text{Si}$	127.54	239.69
$^{132}\text{Sn}+^{87}\text{Se}+^{33}\text{Si}$	155.70	233.68	$^{136}\text{Te}+^{84}\text{Ge}+^{33}\text{Si}$	128.61	233.21
$^{132}\text{Sn}+^{86}\text{Se}+^{34}\text{Si}$	152.26	242.57	$^{134}\text{Te}+^{84}\text{Ge}+^{34}\text{Si}$	124.35	237.34
$^{134}\text{Te}+^{83}\text{Ge}+^{35}\text{Si}$	155.72	234.47	$^{133}\text{Sb}+^{84}\text{Ge}+^{35}\text{P}$	127.10	237.92

Equatorial configuration			Collinear configuration		
Fragmentation channel	V(η) (MeV)	Q value (MeV)	Fragmentation channel	V(η) (MeV)	Q value (MeV)
$^{134}\text{Te}+^{82}\text{Ge}+^{36}\text{Si}$	152.86	237.22	$^{134}\text{Te}+^{82}\text{Ge}+^{36}\text{Si}$	124.88	237.22
$^{133}\text{Sb}+^{82}\text{Ge}+^{37}\text{P}$	155.90	239.48	$^{133}\text{Sb}+^{82}\text{Ge}+^{37}\text{P}$	123.83	239.48
$^{132}\text{Sn}+^{82}\text{Ge}+^{38}\text{S}$	155.76	244.79	$^{134}\text{Te}+^{80}\text{Zn}+^{38}\text{S}$	124.25	238.81
$^{131}\text{Sn}+^{82}\text{Ge}+^{39}\text{S}$	157.76	237.47	$^{134}\text{Te}+^{79}\text{Zn}+^{39}\text{S}$	125.44	236.77
$^{134}\text{Te}+^{78}\text{Zn}+^{40}\text{S}$	154.47	240.69	$^{134}\text{Te}+^{78}\text{Zn}+^{40}\text{S}$	121.73	240.69
$^{134}\text{Te}+^{77}\text{Zn}+^{41}\text{S}$	157.69	237.37	$^{133}\text{Sb}+^{78}\text{Zn}+^{41}\text{Cl}$	124.62	240.85
$^{134}\text{Te}+^{76}\text{Zn}+^{42}\text{S}$	155.34	239.70	$^{132}\text{Sn}+^{78}\text{Zn}+^{42}\text{Ar}$	123.04	245.37
$^{133}\text{Sb}+^{76}\text{Zn}+^{43}\text{Cl}$	157.73	242.16	$^{133}\text{Sb}+^{76}\text{Zn}+^{43}\text{Cl}$	123.80	242.16
$^{132}\text{Sn}+^{76}\text{Zn}+^{44}\text{Ar}$	156.76	247.83	$^{134}\text{Te}+^{74}\text{Ni}+^{44}\text{Ar}$	120.61	241.11
$^{131}\text{Sn}+^{76}\text{Zn}+^{45}\text{Ar}$	157.91	246.44	$^{134}\text{Te}+^{73}\text{Ni}+^{45}\text{Ar}$	121.83	240.14
$^{134}\text{Te}+^{72}\text{Ni}+^{46}\text{Ar}$	154.55	244.24	$^{134}\text{Te}+^{72}\text{Ni}+^{46}\text{Ar}$	118.02	244.24
$^{133}\text{Sb}+^{72}\text{Ni}+^{47}\text{K}$	157.22	241.56	$^{133}\text{Sb}+^{72}\text{Ni}+^{47}\text{K}$	119.18	245.88
$^{134}\text{Te}+^{70}\text{Ni}+^{48}\text{Ar}$	155.81	243.02	$^{132}\text{Sn}+^{72}\text{Ni}+^{48}\text{Ca}$	115.93	251.84
$^{131}\text{Sn}+^{72}\text{Ni}+^{49}\text{Ca}$	157.44	250.07	$^{131}\text{Sn}+^{72}\text{Ni}+^{49}\text{Ca}$	117.60	250.07
$^{132}\text{Sn}+^{70}\text{Ni}+^{50}\text{Ca}$	155.07	252.48	$^{132}\text{Sn}+^{70}\text{Ni}+^{50}\text{Ca}$	115.90	252.48
$^{131}\text{Sn}+^{70}\text{Ni}+^{51}\text{Ca}$	157.43	249.94	$^{131}\text{Sn}+^{70}\text{Ni}+^{51}\text{Ca}$	118.38	249.94
$^{130}\text{Sn}+^{70}\text{Ni}+^{52}\text{Ca}$	157.68	249.56	$^{134}\text{Te}+^{68}\text{Fe}+^{52}\text{Ca}$	117.88	243.36
$^{133}\text{Sb}+^{66}\text{Fe}+^{53}\text{Sc}$	160.96	244.49	$^{133}\text{Sb}+^{66}\text{Fe}+^{53}\text{Sc}$	119.34	244.49
$^{132}\text{Sn}+^{66}\text{Fe}+^{54}\text{Ti}$	159.72	249.72	$^{132}\text{Sn}+^{66}\text{Fe}+^{54}\text{Ti}$	116.58	249.72
$^{131}\text{Sn}+^{66}\text{Fe}+^{55}\text{Ti}$	162.32	246.91	$^{131}\text{Sn}+^{66}\text{Fe}+^{55}\text{Ti}$	119.31	246.91
$^{130}\text{Sn}+^{66}\text{Fe}+^{56}\text{Ti}$	161.83	247.23	$^{134}\text{Te}+^{62}\text{Cr}+^{56}\text{Ti}$	118.87	239.64
$^{131}\text{Sn}+^{64}\text{Fe}+^{57}\text{Ti}$	165.13	244.14	$^{133}\text{Sb}+^{62}\text{Cr}+^{57}\text{V}$	120.38	240.55
$^{134}\text{Te}+^{60}\text{Cr}+^{58}\text{Ti}$	163.76	238.81	$^{132}\text{Sn}+^{62}\text{Cr}+^{58}\text{Cr}$	117.69	245.55
$^{133}\text{Sb}+^{60}\text{Cr}+^{59}\text{V}$	165.56	240.82	$^{131}\text{Sn}+^{62}\text{Cr}+^{59}\text{Cr}$	120.53	242.62
$^{132}\text{Sn}+^{60}\text{Cr}+^{60}\text{Cr}$	162.83	247.17	$^{132}\text{Sn}+^{60}\text{Cr}+^{60}\text{Cr}$	116.87	247.17
$^{130}\text{Sn}+^{61}\text{Cr}+^{61}\text{Cr}$	165.63	242.04	$^{130}\text{Sn}+^{61}\text{V}+^{61}\text{Mn}$	121.32	239.49
$^{128}\text{Sn}+^{62}\text{Cr}+^{62}\text{Cr}$	167.35	242.09	$^{128}\text{Sn}+^{62}\text{Cr}+^{62}\text{Cr}$	120.91	242.09
$^{126}\text{Cd}+^{63}\text{Mn}+^{63}\text{Mn}$	173.23	242.75	$^{125}\text{Cd}+^{64}\text{Cr}+^{63}\text{Fe}$	125.64	240.60
$^{110}\text{Mo}+^{78}\text{Zn}+^{64}\text{Fe}$	172.74	243.00	$^{124}\text{Cd}+^{64}\text{Cr}+^{64}\text{Fe}$	123.16	243.00
$^{109}\text{Mo}+^{78}\text{Zn}+^{65}\text{Fe}$	176.15	245.44	$^{121}\text{Pd}+^{66}\text{Fe}+^{65}\text{Fe}$	128.60	245.44
$^{104}\text{Zr}+^{82}\text{Ge}+^{66}\text{Fe}$	173.07	258.73	$^{120}\text{Pd}+^{66}\text{Fe}+^{66}\text{Fe}$	125.81	248.18
$^{103}\text{Zr}+^{82}\text{Ge}+^{67}\text{Fe}$	174.81	256.91	$^{117}\text{Pd}+^{68}\text{Fe}+^{67}\text{Fe}$	128.83	244.31
$^{102}\text{Zr}+^{82}\text{Ge}+^{68}\text{Fe}$	173.11	258.59	$^{104}\text{Zr}+^{80}\text{Zn}+^{68}\text{Ni}$	126.76	259.02
$^{102}\text{Zr}+^{81}\text{Ge}+^{69}\text{Co}$	174.62	257.80	$^{109}\text{Mo}+^{74}\text{Ni}+^{69}\text{Ni}$	127.87	253.29
$^{102}\text{Zr}+^{80}\text{Zn}+^{70}\text{Ni}$	172.00	260.96	$^{102}\text{Zr}+^{80}\text{Zn}+^{70}\text{Ni}$	124.72	260.96



The relative yield corresponding to equatorial emission lies above the relative yield corresponding to the collinear emission of fragments up to third fragments with mass number $A_3 = 38$ and beyond that the yield corresponding to collinear emission lies well above the relative yield of equatorial emission.

Light fragments prefer the equatorial emission and the heavy fragments prefer the collinear emission.

In particular the relative yield corresponding to the fragment ^{48}Ca and its neighboring nuclei is larger in collinear emission.



THANK YOU

